ISSN 0036-0244, Russian Journal of Physical Chemistry A, 2023, Vol. 97, No. 9, pp. 1871–1879. © Pleiades Publishing, Ltd., 2023.
Russian Text © The Author(s), 2023, published in Zhurnal Fizicheskoi Khimii, 2023, Vol. 97, No. 9, pp. 1239–1247.

CHEMICAL KINETICS AND CATALYSIS

Using Immobilized Hybrid Composites Based on Mixed Polyoxometalates As Catalysts for the Oxidation of Heteroatomic Compounds

V. M. Zelikman[a], K. I. Maslakov[a], I. A. Ivanin[a], and I. G. Tarkhanova[a,*]

[a] *Faculty of Chemistry, Moscow State University, Moscow, 119991 Russia*

**e-mail: itar_msu@mail.ru*

Received March 22, 2023; revised March 22, 2023; accepted March 29, 2023

Abstract—A set of silica gel-immobilized compounds is synthesized that consists of ethylimidazole cations and anions of phosphotungstic acid (lacunar (PW_{11}) or mixed ($PW_{11}M$), where M = Zn, Ni, Cu, Co, Mn). The composition and textural characteristics of the compounds are determined by physicochemical means (IR spectroscopy, XPS, SEM/EDX, adsorption). The synthesized heterogeneous composites are active in the oxidation of sulfur- and nitrogen-containing components of petroleum feedstocks with hydrogen peroxide. A comparative analysis is performed of the samples' catalytic properties in the oxidation of both individual substrates (thiophene, dibenzothiophene, methyl phenyl sulfide, pyridine) and their mixtures.

Keywords: oxidative desulfurization, oxidative denitrogenation, polyoxometalates, immobilized catalysts

DOI: 10.1134/S0036024423090273

INTRODUCTION

Environmental requirements for the content of heteroatomic compounds in petroleum feedstocks (sulfur derivatives in particular) are becoming increasingly stringent, and the potential of the main way of removing these compounds (hydrogenation) is almost exhausted [1]. Oxidative desulfurization (ODS) of petroleum feedstocks is an alternative or supplementary way of hydrotreating. The interest in this option observed in recent years is primarily due to deterioration of the quality of produced oil, due especially to the high content of heavy polyaromatic sulfur-containing derivatives, which are difficult to remove in ways that involve hydrogen [2]. Due to features of the mechanisms of the above two processes, these compounds are quite easily removed via oxidation [3]. It was proposed in [4, 5] that different peroxides (hydrogen peroxide in particular) be used as oxidizing agents. Oxygen is used less frequently because it requires more severe conditions, and ODS technology creates fire and explosion hazards. Since hydrogen peroxide is freely available and environmentally friendly, it is considered the most promising reagent for the practical use of oxidation [6]. Typical catalysts for the process are Brønsted acids and derivatives of groups IV–VI metals in the form of oxides or polyoxometalates (POMs). The process is in two stages because it is necessary to ensure, along with oxidation, the removal of the products—sulfoxides and sulfones—via extraction or adsorption. These functions can be performed simultaneously by specially selected ionic liquids that contain acid sites and/or derivatives of a number of transition metals [7]. To increase the area of contact with the reaction solution and reduce their consumption, ionic liquids are commonly deposited on the surfaces of supports to form hybrid heterogeneous composites that can also act as adsorbents [8].

In addition to sulfur-containing heteroatomic compounds, petroleum feedstocks comprise such nitrogen-containing compounds as pyridine and indole derivatives, which are catalytic poisons in many oil refining processes. Regulatory requirements for the content of nitrogen oxides in exhaust gases have been severely tightened in recent years [9], further stimulating the search for new ways of removing the above compounds that can be used instead of or in combination with means that involve hydrogen [10]. According to some authors, oxidative denitrogenation occurs more readily than ODS when the same catalysts are used [11]. Most ODS catalysts therefore ensure the exhaustive oxidation of heteroatomic compounds of both classes or the preferential oxidation of nitrogen derivatives. On the other hand, the content of nitrogen in some petroleum products is regulated less strictly than that of sulfur (less than 10 ppm), so in some cases there is no need to remove them completely. This allows the untargeted consumption of the oxidizing agent to be reduced. Deliberately designing catalysts that correspond to a specific task in the purification of

petroleum feedstocks is therefore a problem of great interest.

In our previous papers [12–14] it was shown that SiO_2-immobilized imidazole derivatives of phosphomolybdic and phosphotungstic heteropoly acids were active catalysts for the oxidation of sulfur-containing compounds. It is known from the literature that altering the structure of a heteropoly acid anion by introducing transition metal ions affects the redox potential of the anion. This is apparent from, e.g., a change in the activity of the respective catalysts in the oxidation of alcohols [15]. In these composites, the possibility of coordination with respect to different heteroatomic compounds will obviously change as well and affect the rate of their oxidation. Imidazole derivatives with $[PW_{11}(M{\cdot}OH_2)O_{39}]^{5-}$ (where M = Zn, Ni, Co, Mn, Cu) anions were therefore chosen as catalysts, and analogous derivatives with a lacunar anion were used for comparison. Activity in the oxidation of sulfur-containing derivatives has been shown in the literature for a number of catalysts containing active sites with similar structure, but the composition of those composites and the way of synthesizing them differed from those we have proposed (using imidazolium cations covalently bonded to a surface of silica gel) [16–19]. The choice of thiophene, methyl phenyl sulfide, and dibenzothiophene (DBT) as model substrates is due to their presence in light oil fractions and motor fuels. In addition, thiophene is the aromatic sulfur-containing compound most difficult to oxidize [20]. Pyridine was chosen as an example of a nitrogen-containing substrate because it is capable of strong complexation and thus a poison for many metal-containing catalysts. Since pyridine is a stronger base, it can also block the acid sites of heterogeneous catalysts and thus create still more difficulties in the adsorption and subsequent oxidation of sulfur-containing substrates.

The aim of this work was therefore a comparative analysis of the catalytic properties of immobilized imidazole derivatives of the above heteropoly compounds in the oxidation of sulfur- and nitrogen-containing compounds (individually and as part of a mixture) with hydrogen peroxide in an isooctane solution.

EXPERIMENTAL

Reagents and materials. The following reagents were used to synthesize our catalysts: $Ni(NO_3)_2{\cdot}6H_2O$ (Fluka, >99%), $Zn(CH_3COO)_2{\cdot}2H_2O$ (Fluka, >99%), $Co(NO_3)_2{\cdot}6H_2O$ (Fluka, >98%), $Mn(CH_3COO)_2{\cdot}4H_2O$ (Fluka, >99%), $CuCl_2{\cdot}2H_2O$ (Fluka, >99%), $Na_2HPO_4{\cdot}H_2O$ (reagent grade, Khimmed), $Na_2WO_4{\cdot}2H_2O$ (analytical grade, Reakhim), hydrochloric acid (37% HCl, reagent grade), potassium chloride KCl (reagent grade, Reakhim), ethanol (rectified, 95%), methanol (Merck, >99.8%), isooctane (99.5%, reagent grade), 3-chloropropyltrimethoxysilane (CPTMS; 99.5%, Fluka), ethylimidazole (99%, Fluka), and hydrogen peroxide (30%, LLC Prime Chemicals Group). Thiophene (Fluka, >98%), DBT (Fluka, >98%), methyl phenyl sulfide (thioanisole) (analytical grade, Reakhim), and pyridine (Fluka, >99%) were used as substrates for oxidation. Isooctane (special purity grade, Reakhim) was used as a solvent. All of the above reagents were introduced into the reaction without further purification.

A Perlkat-97-0 silica gel (fraction, 1–3 mm; specific surface area, $S_{sp} = 500$ m^2/g; effective pore diameter, $d_{pore} = 10$ nm, BASF) was used as a support for synthesizing our catalysts. The preconditioning of the support in synthesizing the catalysts is described below.

Catalyst Synthesis Procedure

Preconditioning and surface modification of the support. Surface of silica gel was treated as described in [21] (Fig. 1). Physically bound water was removed from the surfaces via azeotropic distillation. A round-bottom flask equipped with a Dean–Stark trap with a reflux condenser was used to heat the required weighed portion of silica gel with stirring under a layer of boiling toluene, until the volume of water in the trap stopped growing. The trap was then removed, and the reflux condenser was attached directly to the flask. CPTMS was added to the contents of the flask in a molar ratio of 1 : 1 to the determined number of silanol groups on the surface of the support, and boiling with stirring continued for 24 h. The contents of the flask were discarded on a filter when boiling was complete. The solid was washed three times with dry toluene and allowed to dry in air at room temperature.

The quaternization of *N*-ethylimidazole with a chlorine derivative grafted onto the silica gel surface began with placing a 10-g weighed portion of the modified support into a 50-mL glass tube. *N*-Ethylimidazole was added until the solid mass was completely impregnated. The tube was evacuated to 10^{-2} Torr while cooling with liquid nitrogen. It was then sealed off and placed in a thermostat for 12 h at 160°C.

When the heating stage was complete, the tube was cooled to room temperature and opened. The solid phase was transferred to a glass beaker and washed twice (in 15-mL portions) with ethanol and then three times (in 30-mL portions) with diethyl ether to remove unreacted *N*-ethylimidazole. The resulting modified supports were dried in a vacuum.

Lacunar compound synthesis. Lacunar POM $K_7[PW_{11}O_{39}]{\cdot}12H_2O$ (referred to below as PW) was synthesized according the procedure proposed in [22]:

$$11Na_2WO_4 + Na_2HPO_4 + 7KCl + 17HCl = K_7PW_{11}O_{39} + 24NaCl + 9H_2O.$$

Under vigorous stirring, 18.2 g (0.055 mol) of $Na_2WO_4{\cdot}2H_2O$ and 0.93 g (0.0052 mol) of

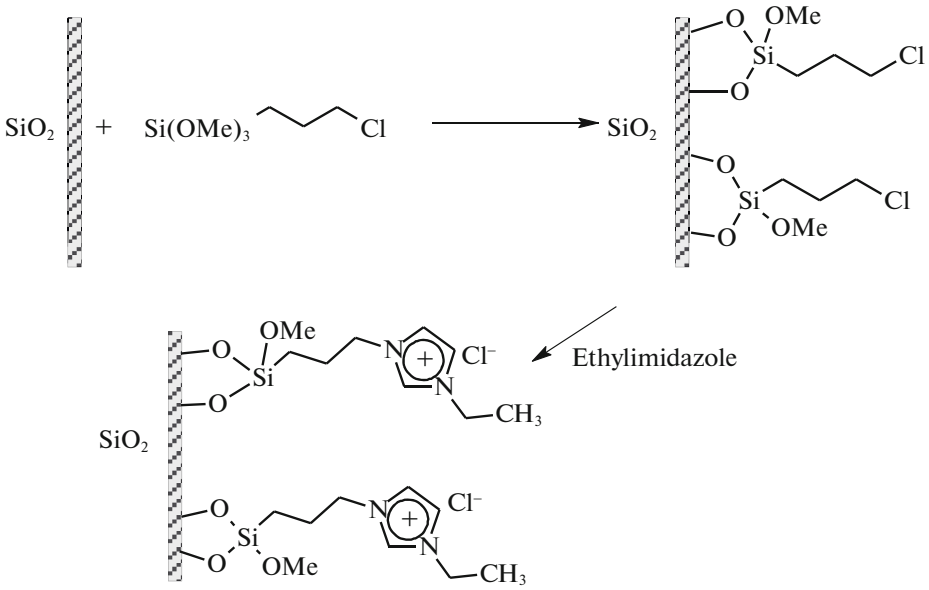

Fig. 1. Schematic modification of a silica gel surface with an imidazole derivative.

$Na_2HPO_4 \cdot H_2O$ were added to 30 mL of deionized water placed in a reactor thermostated at 95°C. Once the salts had dissolved completely, 20 mL of 4 M HCl was gradually added to the resulting solution using a dropping funnel. Once the acid was introduced, the resulting solution was thermostated with stirring for 1 h. Then 7.5 g of KCl was added, and the resulting mixture was stirred for another 10 min. The still hot solution was filtered off next, and the resulting filtrate was evaporated on a rotary evaporator until a white turbidness appeared. The solution was transferred to a glass beaker, which was left open at room temperature for several days to ensure the product crystallized in the form of a white needle-like precipitate. The crystals precipitated as the water evaporated and were collected by decanting. The collection of the crystals ceased when the volume of the liquid remaining in the beaker was around 15 mL, since the solution contained mostly sodium chloride. The resulting crystals of the product were recrystallized from hot water, dried at room temperature, and used to synthesize mixed POMs. The yield was 12.36 g (78% of the calculated value).

Mixed POM synthesis. Compounds of $K_5[PW_{11}O_{39}(M \cdot OH_2)]$ (referred to below as PWM, where M = Zn, Ni, Co, Mn, Cu) were synthesized as described in [15]. Using the example of a copper-containing heteropoly compound, 3.00 g (9.4×10^{-4} mol) of PW_{11} was dissolved in 15 mL of deionized water at 80°C, and 0.16 g (9.4×10^{-4} mol) of $CuCl_2 \cdot 2H_2O$ was dissolved separately in 10 mL of deionized water at 80°C. The solutions were then mixed and stirred vigorously for 1 h at 80°C. The resulting transparent yellow solution was cooled to room temperature, and 50 mL of a methanol–ethanol mixture in a volume ratio of 1 : 1 was added to the solution. The resulting yellow-green precipitate was filtered off, washed with methanol, and dried at room temperature.

Polyoxometalate immobilization. Surface-bound POMs were synthesized with stirring. Using the example of Cu, 0.51 g of PWCu was dissolved in 5 mL of deionized water heated to 85°C. Silica gel granules with a total weight of 1.54 g were introduced into the resulting transparent solution without interrupting the stirring. The particles were allowed to interact for 6 h at 85°C and then for 12 h at room temperature with continuous stirring. The blue granules (referred to below as PWCu_s) were then removed from the reaction vessel, washed with small amounts of deionized water, and dried in air (Fig. 2).

Investigations. Infrared (IR) spectra in KBr pellets were recorded on an Infralum FT-801 Fourier transform IR spectrophotometer in the range of 4000–400 cm^{-1}. The analyte was ground in a mortar with anhydrous KBr in a ratio of 1 : 85 and then compressed into tablets.

The surfaces of the catalyst samples were studied on a JSM-6000 NeoScope scanning electron microscope (JEOL, Japan) with a built-in EX-230 X-ray analyzer for energy dispersive X-ray (EDX) analysis. The images were recorded in the high-vacuum mode at an accelerating voltage of 15 kV. Signals were detected in the secondary electron imaging mode.

The texturural parameters of the catalysts were determined via low-temperature nitrogen adsorption on an Autosorb1 analyzer (Quantachrome, United States). The samples were preliminarily evacuated for 3 h at 150°C. The textural parameters of the catalysts

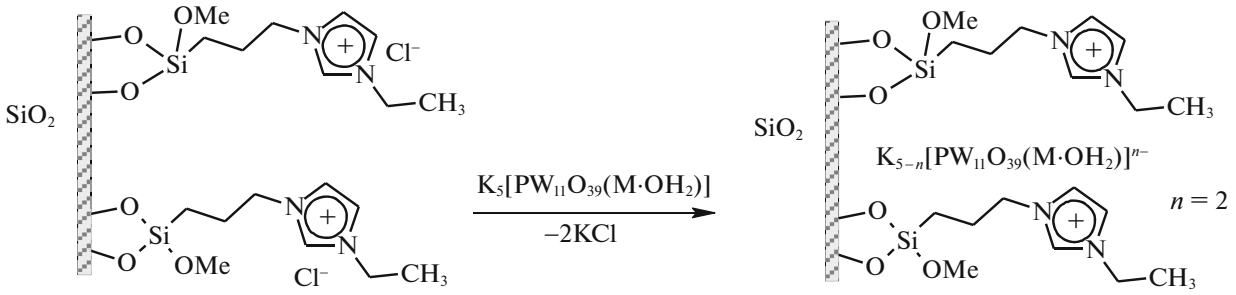

Fig. 2. Schematic immobilization of POMs when $n = 2$.

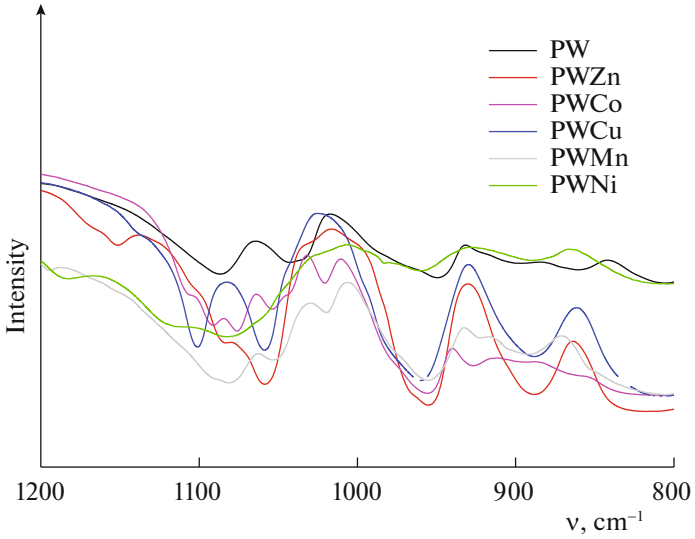

Fig. 3. Infrared spectra of the POMs.

were calculated with the Brunauer–Emmett–Teller (BET) and Barrett–Joyner–Halenda (BJH) models using the analyzer software package.

X-ray photoelectron (XP) spectra of the catalysts were recorded on an Axis Ultra DLD spectrometer (Kratos Analytical, United Kingdom) using monochromatic AlK_α radiation. The spectra were recorded at a pass energy of the analyzer of 160 (survey spectra) and 40 eV (high-resolution spectra). A neutralizer was used in recording the spectra, which were calibrated against the low-energy component of the C 1*s* spectrum. The bonding energy of the spectra was assumed to be 285.0 eV.

Catalytic oxidation of heteroatomic substrates. To start the oxidation reaction, 10 mL (1 wt %) of a substrate solution in isooctane (or a solution of a mixture of two substrates with a 0.5% weight fraction of each component), the catalyst (0.1 g), and an oxidizing agent (H_2O_2, 0.4 mL) were placed into a jacketed reactor with a magnetic stirrer. The contents of the reactor were stirred under heating (60°C). At regular intervals, samples of the reaction solution were taken for analysis via gas–liquid chromatography on a Kristall-2000 instrument equipped with a Zebron ZB-1 capillary column (30 m) and a flame ionization detector. The conversion of substrates was measured from the drop in their concentration in the hydrocarbon phase, according to an internal standard (nonane or dodecane).

RESULTS AND DISCUSSION

Physicochemical properties of the synthesized catalysts. Fourier transform IR spectra of the synthesized catalysts are presented in Fig. 3. According to [22], the spectrum of phosphotungstic acid $H_3[PW_{12}O_{40}]$ with a Keggin structure displays a characteristic band in the region of 1080 cm^{-1} that was attributed to the asymmetric vibrations of the P–O bonds.

Two bands can be seen in the spectra of $K_7[PW_{11}O_{39}]$ in the region of 1000–1100 cm^{-1}. The emergence of lacunes in the $[PW_{11}O_{39}]^{7-}$ heteropoly anions reduced the symmetry of the central PO_4 moiety, so the P–O band was split (see the spectrum of

Table 1. Splitting of the P–O bands in the IR spectra of POMs

POM	Position of the P–O band, cm^{-1}	Splitting of the P–O band, cm^{-1}
PW	1086	44
PW Zn	1085	27
PWCu	1101	43
PWNi	1084	44
PWCo	1091	?
PWMn	1081	32

PW) in agreement with the data in [15]. Incorporating a transition metal into the structure of the $[PW_{11}O_{39}(M{\cdot}OH_2)]^{5-}$ monolacunary heteropoly anions more or less restored the symmetry of the central PO_4 moiety. This reduced the splitting of the band attributed to P–O, which depended on the nature of the metal ions (Fig. 3, Table 1). The degree of splitting was reduced considerably for Zn- and Mn-containing PWs, but it remained the same for PWNi and PWCu. Several bands appeared in this region for Co, so the degree of splitting could not be determined correctly.

The presented spectra also display bands attributed to the bonds of W with terminal oxygen atoms $W{=}O_t$ (at ~950 cm^{-1}), corner-sharing $W{-}O_c{-}W$ (at ~885 cm^{-1}), or edge-sharing $W{-}O_e{-}W$ bridging bonds (at 800 cm^{-1}), the positions of which are in good agreement with those described in [14].

Results from our XPS studies of the catalyst samples are presented in Table 2. In addition to the main doublet with a bonding energy of 35.8–36.1 eV for the W 4*f* component (corresponding to the +6 state of tungsten oxidation), the W 4*f* XP spectra of the samples (except for PWCu) exhibit a W 4*f* component with a bonding energy of 34.0–34.6 eV that was attributed to W^{4+}, the emergence of which was due to the partial reduction of tungsten under the conditions of the spectrometer [23]. The apparent bonding energy of the P 2*p* line (133.6–134.2 eV) can be attributed to the oxidized state of phosphorus in the composition of the heteropoly anions [23–26]. The O 1*s* spectra indicate there was a W–O–P or W–O–H bond with an energy of around 532.7 eV [23, 27] and a W–O–W bond with an energy of around 530.6 eV [26–29]. The line at 532.5 eV can also be attributed to Si–O–Si bonds [1, 3, 30].

The XP spectra of samples with supported POMs display M 2*p* lines, confirming the presence of metals in respective states of oxidation on their surfaces.

The morphology of the catalyst samples was characterized via scanning electron microscopy (SEM). Figure 4 shows images of the surface of the catalysts with (a) PW_s and (b) PWNi_s. It is clear that the surfaces of the samples had a loose rough structure, on which we can see fragments of the active phase that formed.

Results from our EDX analysis of samples with supported POMs are presented in Fig. 5. It is clear that the zinc, nickel, cobalt, manganese, and copper atoms were distributed quite uniformly over most of the analyzed surface of the support.

Table 2. Results from XPS analysis of our heterogeneous samples

POM sample	Content of element, at % (bonding energy, eV)					
	metal	O 1*s*	N 1*s*	P $2p_{3/2}$	Si 2*p*	W 4*f*
(PW)_s	—	13.9 (530.7) 38.0 (532.7)	0.5 (399.6) 3.8 (401.7)	0.2 (133.6)	16.1 (103.6)	0.2 (34.6) 3.2 (35.9)
(PWZn)_s	0.2 (1021.7) Zn $2p_{3/2}$	8.4 (530.4) 43.4 (532.7)	0.8 (399.7) 3.2 (401.7)	0.3 (133.7)	20.2 (103.6)	0.1 (34.2) 2.2 (35.7)
(PWCu)_s	1.13 (933.0) 0.68 (934.5) Cu 2*p*	23.0 (530.7) 7.3 (532.1) 2.3 (533.1)	3.3 (399.6) 4.6 (400.9) 0.5 (403.0)	0.8 (133.9)	16.3 (103.1)	7.6 (35.8)
(PWNi)_s	1.37 (855.9) Ni $2p_{3/2}$	19.1 (530.6) 23.0 (532.7)	1.6 (399.6) 6.2 (411.6)	0.6 (134.1)	18.6 (103.6)	0.1 (34.0) 5.4 (35.8)
(PWCo)_s	≤0.03 (781.4) Co $2p_{3/2}$	2.3 (530.6) 55.1 (532.7)	0.1 (399.3) 0.2 (400.2) 0.1 (401.8)	0.1 (134.1)	25.4 (103.6)	0.1 (34.6) 0.54 (36.1)
(PWMn)_s	0.04 (641.4) Mn $2p_{3/2}$	1.4 (530.5) 52.6 (532.8)	0.2 (399.7) 0.1 (401.4)	≤0.1 (134.2)	24.3 (103.6)	≤0.1 (34.5) 0.4 (35.9)

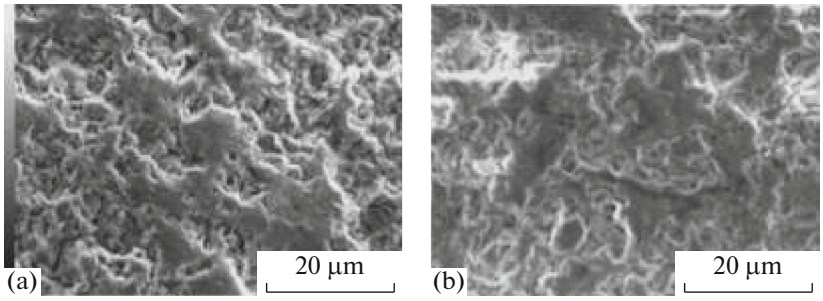

Fig. 4. Scanning electron microscope images of the surfaces of samples: (a) (PWNi)_s and (b) (PW)_s.

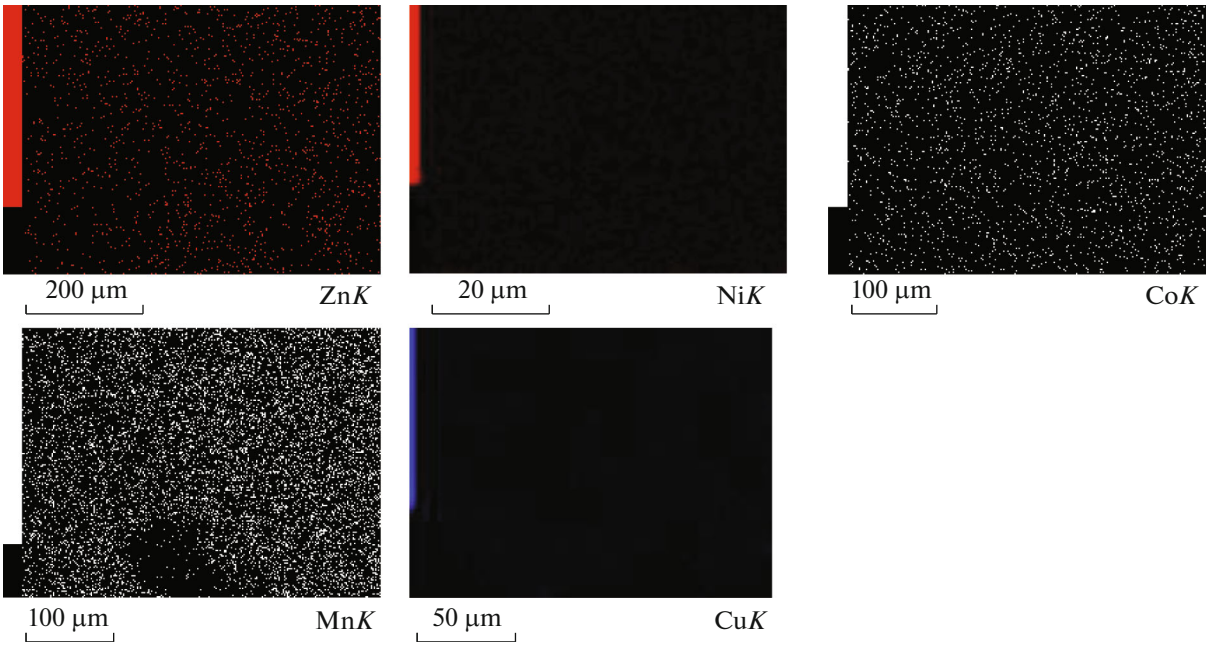

Fig. 5. Maps of the distribution of metals on the surfaces of the respective (PWM)_s catalysts, according to EDX.

The sites of P and W localization largely coincide, confirming they were bound into the chemical compound. Surface mapping of the samples revealed a mostly uniform distribution of metal atoms relative to W and P atoms, testifying to the uniform distribution of heteropoly anions over the surfaces of the support.

The ratio between K and Na atoms, determined from SEM/EDX data, suggests that sodium cations were displaced almost completely from the POM during the synthesis of the heteropoly compounds. The predominance of N atoms over Cl atoms in the analyzed samples, which was revealed by XPS, indicates chloride anions were largely replaced by heteropoly anions during the synthesis of the immobilized derivatives.

Table 3 gives the textural parameters and content of tungsten in the catalysts.

We can see the POM-modified silica gel had smaller specific surface areas and volumes of pores than those of the original silica gel. The change in the average pore diameter suggests the coating was nearly a monolayer in most of the samples.

Catalysis. Processing the temporal dependences of the substrates' oxidative conversion produced effective constants of the reaction (see Table 4). The pseudo-first-order constants of the reaction rate were determined using the equation $r_0 = k[S]_0$, where $[S]_0$ is the initial concentration of the substrate, since it is known from the literature that this equation describes the oxidation of sulfur-containing compounds with H_2O_2 in nonpolar media when solid catalysts are used [32].

Analysis of these data suggests that the highest rates of the oxidation of heterocyclic sulfur-containing compounds were observed for (PWZn)_s and (PWCu)_s. Slightly lower values were observed when

Table 3. Composition and textural characteristics of our catalysts

Catalyst	[W], wt %	S ($m^2 g^{-1}$)	D_{pore} (nm)	V_{pore} (cm^3/g)
SiO_2	0	300	9	0.69
(PW)_s	14	167	8.2	0.44
(PWZn)_s	12	152	7.4	0.41
(PWCu)_s	15	176	8.1	0.49
(PWNi)_s	19	142	8.2	0.40
(PWCo)_s	7	274	8.2	0.66
(PWMn)_s	5	290	8.1	0.63

[W] is the content of W according to SEM/EDX, S is the specific surface area (BET), D_{pore} is the average pore diameter (BJH), and V_{pore} is the pore volume (BJH).

using (PWNi)_s. The relatively high activity of these catalysts can be attributed to the tendency of the metal ions contained in the catalysts to form complexes with S-containing aromatic substrates. However, the formation of these complexes with low bonding energies [33] was probably one of the initial stages of oxidation. The lower results from catalysts with the participation of Co and Mn ions were apparently due to the relatively low numbers of metal ions on their surfaces. At the same time, the (PW)_s catalyst species with no second metal displayed low activity in reactions with thiophene and a thiophene derivative, in contrast to methyl phenyl sulfide. We may assume that when a lacunar compound is used, oxidation proceeds according to a mechanism that differs from the pathway of the reaction with the participation of bimetallic catalysts [34, 35]. This hypothesis is supported by the considerable difference between the constants of the rate of DBT oxidation and those of thiophene oxidation for a lacunar POM, compared to samples of the Mn- and Co-containing catalysts in which there were few metal ions and the number of lacunar moieties in the composition of the ionic liquid anions immobilized on the surface was considerable.

An opposite picture was observed in analyzing the results from pyridine oxidation. The highest rate of the reaction was observed when using the lacunar system. Oxidation proceeded more slowly when there were other POMs. We may assume that with metal-containing catalysts, the process at the initial stage proceeds through the formation of complexes of metal ions with the nitrogen contained in pyridine, as discussed above for S-containing compounds. The high strength of the resulting complexes and the tendency of pyridine to form multiligand complexes with transition metal ions [36], which reduces the accessibility of the active sites of the catalyst, can apparently slow the development of the oxidation process.

Table 4. Effective oxidation rate constants of the substrates (k_{eff}^{I}, 1/h)

Catalyst	Thiophene	DBT	Thioanisole	Pyridine
(PW)_s	0.16	0.36	0.99	1.24
(PWZn)_s	0.46	0.42	1.50	0.84
(PWCu)_s	0.56	0.43	0.65	0.54
(PWNi)_s	0.26	0.33	0.97	0.51
(PWCo)_s	0.20	0.25	0.60	0.51
(PWMn)_s	0.16	0.22	0.36	0.65

To model a process that can be implemented when nitrogen- and sulfur-containing compounds are in light oil feedstocks simultaneously, tests on the simultaneous oxidation of heteroatomic substrates (thiophene and pyridine) were performed for catalysts that showed good results. Our test results are presented in Fig. 6.

It should be noted that the depths of oxidation of pyridine within 4 h were similar for all four catalysts when this substrate was used individually or as part of a mixture, although the behavior of the curves could differ at shorter times. The behaviors of the curves are thus almost identical for catalysis with PW_{11} (i.e., thiophene in the mixture had no effect on the oxidation of pyridine). However, the rate of thiophene oxidation in a mixture was higher than in an individual solution.

Similar dependences of the oxidation of the two substrates were observed for our (PWCu)_s and (PWZn)_s catalysts. The oxidation of pyridine in a mixture proceeded somewhat more slowly than it did in individual solutions. However, the depths of the reaction were identical after 4 h (for Cu) or differed only slightly (for Zn). For these catalyst systems, the second substrate in the solution had a quite different effect on the oxidation of thiophene, which it slowed considerably (by 10–15%). This effect can be attributed to large amounts of metal-containing catalyst species participating in complexation with several pyridine molecules, which lowered the content of catalytically active particles capable of forming products of thiophene oxidation (i.e., the depth of the reaction was reduced).

For oxidation using (PWNi)_s as a catalyst, a single case was observed in which the rate of the process at the initial stage of the reaction with individual pyridine was lower than in a mixture of substrates. This finding can be attributed to the transition metal bonding into low-activity complexes in parallel with the reaction (even more vigorously than the bonding of the copper-containing catalyst), slowing its rate. Being with pyridine simultaneously did not affect the rate of thiophene oxidation appreciably, at least for the first three hours. The behaviors of the two curves were

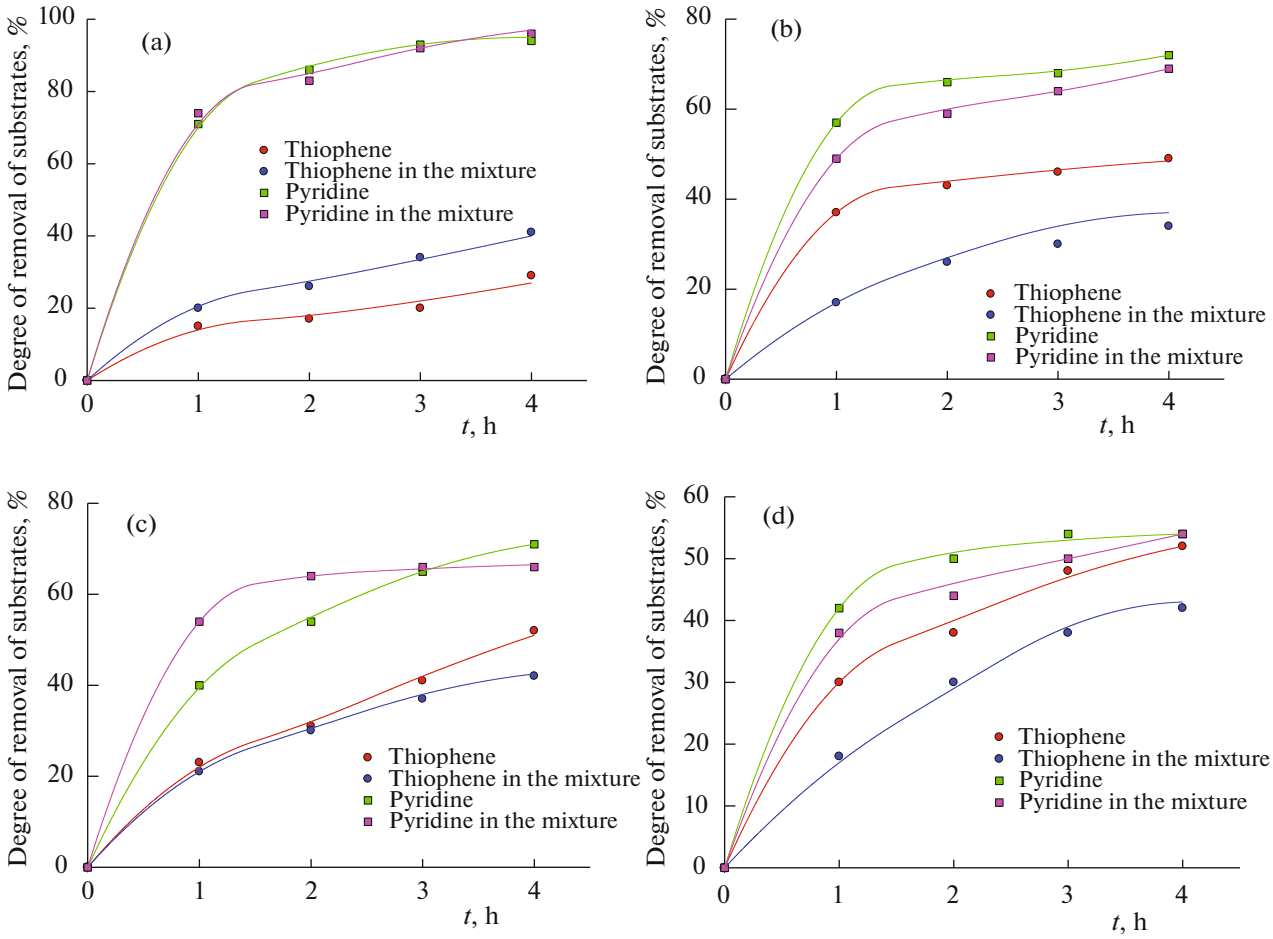

Fig. 6. Removal of substrates versus time with catalysts: (a) (PW)_s, (b) (PWZn)_s, (c) (PWNi)_s, and (d) (PWCu)_s.

almost identical during this period, after which the depth of thiophene oxidation fell slightly when the nitrogen-containing compound was used. This could indicate the nickel derivative was effectively bound with thiophene into a catalytically active complex, regardless of possible competing complexation.

CONCLUSIONS

The simultaneous presence of two substrates affected the activity of all our catalysts. The effect thiophene had on the rate of denitrogenation was much weaker than the opposite effect. We believe this can be attributed to pyridine being more prone to complexation with transition metals than thiophene. It is therefore subject to preferential adsorption on the active sites of the catalyst, which inhibits desulfurization. On the other hand, pyridine (a strong base) can participate in the bonding of products of oxidation of sulfur-containing compounds (i.e., sulfonic acids). This effect can be observed for (PW)_s catalyst, where the rate of desulfurization even grows slightly. The combination of these factors must be considered when choosing catalysts required for the specific task of a test.

FUNDING

This work was performed within the framework of the State Assignment to the Lomonosov Moscow State University (project no. AAAA-A21-121011590090-7) on equipment purchased as part of the Program for the Development of Moscow State University.

CONFLICT OF INTEREST

The authors declare that they have no conflict of interest.

REFERENCES

1. A. Tanimu and K. Alhooshani, Energy Fuels **33**, 2810 (2019).
2. R. Shafi and G. J. Hutchings, Catal. Today **59**, 423 (2000).
3. S. Houda, C. Lancelot, P. Blanchard, et al., Catalysts **8**, 344 (2018).

4. I. Shafiq, S. Shafique, P. Akhter, et al., J. Clean. Prod. **294**, 2 (2021).
5. E. A. Eseva, A. V. Akopyan, A. V. Anisimov, and A. L. Maksimov, Pet. Chem. **60**, 979 (2020).
6. A. Rajendran, T. Cui, H. Fan, et al., J. Mater. Chem. A **8**, 2246 (2020).
7. F. Liu, J. Yu, A. B. Qazi, et al., Environ. Sci. Technol. **55**, 1419 (2021).
8. *Ionic Liquids: Theory and Practice, Problems of Chemistry of Solutions,* Ed. by A. Yu. Tsivadze (Ivan. Izdat. Dom, Ivanovo, 2019), p. 672 [in Russian].
9. L. Yang, V. Franco, P. Mock, et al., Environ. Sci. Technol. **49**, 14409 (2015).
10. Z. S. Aghbolagh, M. R. K. Khorrami, and M. S. Rahmatyan, J. Iran Chem. Soc. **19**, 219 (2022).
11. P. de A. Mello, M. A. G. Nunes, C. A. Bizzi, et al., in *Proceedings of the 13th Meeting of European Society of Sonochemistry, 2012,* p. 148.
12. A. G. Ali-Zade, A. K. Buryak, V. M. Zelikman, et al., New J. Chem. **4**, 6402 (2020).
13. A. A. Bryzhin, M. G. Gantman, A. K. Buryak, et al., Appl. Catal. B **257**, 117938 (2019).
14. I. G. Tarkhanova, S. V. Verzhichinskaya, A. K. Buryak, V. M. Zelikman, O. I. Vernaya, R. Z. Sakhabutdinov, R. M. Garifullin, T. V. Bukharkina, and L. A. Tyurina, Kinet. Catal. **58**, 362 (2017).
15. J. H. Choi, J. K. Kim, D. R. Park, and T. H. Kang, J. Mol. Catal. A **371**, 111 (2013).
16. L. S. Nogueira, S. Ribeiro, C. M. Granadeiro, et al., Dalton Trans. **43**, 9518 (2014).
17. A. Patel, N. Narkhede, S. Singh, et al., Catal. Rev.–Sci. Eng. **58**, 337 (2016).
18. J. Li, Zh. Yang, S. Li, et al., J. Ind. Eng. Chem. **82**, 1 (2020).
19. Y. Xu, W.-W. Ma, A. Dolo, et al., RSC Adv. **6**, 66841 (2016).
20. Z. Ismagilov, S. Yashnik, M. Kerzhentsev, et al., Catal. Rev.–Sci. Eng. **53**, 199 (2011).
21. I. G. Tarkhanova, V. M. Zelikman, and M. G. Gantman, Appl. Catal. A **470**, 81 (2014).
22. F. Jonnevijlle, C. M. Tourné, and G. F. Tourné, Inorg. Chem. **21**, 2742 (1982).
23. P. A. Jalil, M. Faiz, N. Tabet, et al., J. Catal. **217**, 292 (2003).
24. J. Li, L. Luo, W. Tan, et al., Environ. Sci. Pollut. Res. **26**, 34248 (2019).
25. M. Imran, X. Zhou, N. Ullah, et al., Chem. Sel. **2**, 8625 (2017).
26. J. L. Fiorio, A. H. Braga, C. L. B. Guedes, et al., ACS Sustain. Chem. Eng. **7**, 15874 (2019).
27. E. I. García-López, G. Marcí, I. Krivtsov, et al., J. Phys. Chem. C **123**, 19513 (2019).
28. J. G. Hernéz-Cortez, M. Manríquez, L. Lartundo-Rojas, et al., Catal. Today **220–222,** 32 (2014).
29. J. Molina, J. Fernandez, A. I. del Rio, et al., Appl. Surf. Sci. **257**, 10056 (2011).
30. D. A. Zatsepin, P. Mack, A. E. Wright, et al., Phys. Status Solidi A **208**, 1658 (2011).
31. A. U. Alam, M. M. R. Howlader, and M. J. Deen, ECS J. Solid State Sci. Technol. **2** (12), 515 (2013).
32. L. Konga, G. Lia, and X. Wang, Catal. Lett. **92b**, 163 (2004).
33. A. L. Maksimov and A. I. Nekhaev, Pet. Chem. **60**, 155 (2020).
34. A. A. Bryzhin, V. S. Rudnev, I. V. Lukiyanchuk, M. S. Vasilyeva, and I. G. Tarkhanova, Kinet. Catal. **61**, 283 (2020).
35. T. N. Rostovshchikova, E. S. Lokteva, M. I. Shilina, E. V. Golubina, K. I. Maslakov, I. N. Krotova, A. A. Bryzhin, I. G. Tarkhanova, O. V. Udalova, V. M. Kozhevin, D. A. Yavsin, and S. A. Gurevich, Russ. J. Phys. Chem. A **95**, 451 (2021).
36. *Pyridine: A Useful Ligand in Transition Metal Complexes,* Ed. by P. P. Pandey (InTech Open, Rijeka, 2018), p. 84.

Translated by M. Timoshinina